Gas-Phase Reactions of Americium Ion, Am^+, with Alkenes

John K. Gibson

Chemical and Analytical Sciences Division, Oak Ridge National Laboratory, Oak Ridge, Tennessee 37831-6375

Received March 3, 1998

The investigation of gas-phase activation of alkene C−H bonds by f-element metal ions has been extended to americium (Am^+) using the technique of laser ablation with prompt reaction and detection; reactions were carried out with ethene, 1-butene, 2-butene, cyclohexene, benzene, 1,5-cyclooctadiene (COD), and cyclooctatetraene (COT). The product $\{Am-L^*\}^+$ compositions and abundances were compared with those for lighter An^+ and Ln^+. For the linear and cyclic C_6 alkene reactants, Am^+ was found to be essentially inert—only a minuscule amount of the $\{Am^+-benzene\}$ condensation product was detected. Reactions with COD and COT produced the dehydrogenation complexes, $\{Am-C_8H_8\}^+$ and $\{Am-C_8H_6\}^+$, though in lower yields than for lighter An^+. Overall, the C−H activation efficacy of Am^+ was smaller than that for the preceding An^+ but was closer to that of the relatively unreactive lanthanide ion Tm^+. This result is interpreted to indicate that the 5f electrons of Am^+, like the 4f electrons of the Ln^+, do not substantially participate in C−H (or C−C) activation. Apparently, ground-state Am^+ with its $[Rn]5f^77s^1$ orbital occupancy must be excited to the $[Rn]5f^66d^17s^1$ state, 245 kJ mol^{-1} above ground, which comprises two chemically active 6d/7s electrons and is capable of forming a C−Am^+−H dehydrogenation intermediate. The greatly enhanced reactivity of Am^+ with COD and COT compared with the smaller alkenes can be rationalized in the context of a "curve-crossing" model for the C−H activation process.

Introduction

Gas-phase organometallic chemistry has emerged as a powerful means to elucidate fundamental transition-metal ion (M^+) to ligand (L) interactions.[1−5] The initial thrust was on the first-row d-block transition elements,[1] but several studies have established this approach for studying C−H and C−C bond activation by f-element lanthanide (Ln^+ and LnO^+)[6−14] and actinide (An^+ and AnO^+)[15−21] ions. In contrast to condensed-phase organolanthanide chemistry,[22,23] free Ln^+ exhibit widely disparate reactivities across the series, which reflect the energies required to excite ground-state Ln^+ to an electronic configuration with two unpaired non-4f valence electrons capable of forming s-type bonds in a C−Ln^+−H intermediate prior to facile H_2 loss. The necessity for promotion of a 4f electron to a reactive 5d valence orbital is consistent with the typically chemically inert character of the spatially localized, low-energy valence 4f electrons.[24]

The 5f orbitals of the light actinides exhibit a greater propensity toward chemical interaction than do the more localized 4f lanthanide orbitals,[25] but the degree of involvement of the 5f electrons in organoactinide bonding remains uncertain.[26] Initial gas-phase organoactinide studies were carried out with Th^+ [18] and U^+,[15−17] which exhibit ground-state configurations with

(1) Eller, K.; Schwarz, H. *Chem. Rev.* **1991**, *91*, 1121−1177.
(2) Weishaar, J. C. *Acc. Chem. Res.* **1993**, *26*, 213-219.
(3) Freiser, B. S. *Acc. Chem. Res.* **1994**, *27*, 353−360.
(4) Organometallic Ion Chemistry; Freiser, B. S., Ed.; Kluwer: Dordrecht, 1996.
(5) Freiser, B. S. *J. Mass Spectrom.* **1996**, *31*, 703−715.
(6) Huang, Y.; Wise, M. B.; Jacobson, D. B.; Freiser, B. S. *Organometallics* **1987**, *6*, 346−354.
(7) Schilling, J. B.; Beauchamp, J. L. *J. Am. Chem. Soc.* **1988**, *110*, 15−24.
(8) Sunderlin, L. S.; Armentrout, P. B. *J. Am. Chem. Soc.* **1989**, *111*, 3845−3855.
(9) Yin, W. W.; Marshall, A. G.; Marcalo, J.; Pires de Matos, A. *J. Am. Chem. Soc.* **1994**, *116*, 8666−8672.
(10) Heinemann, C.; Schroder, D.; Schwarz, H. *Chem. Ber.* **1994**, *127*, 1807−1810.
(11) Cornehl, H. H.; Heinemann, C.; Schroder, D.; Schwarz, H. *Organometallics* **1995**, *14*, 992−999.
(12) Heinemann, C.; Cornehl, H. H.; Schroder, D.; Dolg, M.; Schwarz, H. *Inorg. Chem.* **1996**, *35*, 2463−2475.
(13) Gibson, J. K. *J. Phys. Chem.* **1996**, *100*, 15688−15694.
(14) Cornehl, H. H.; Wesendrup, R.; Harvey, J. N.; Schwarz, H. *J. Chem. Soc., Perkin Trans. 2* **1997**, 2283−2291.
(15) Armentrout, P. B.; Hodges, R. V.; Beauchamp, J. L. *J. Chem. Phys.* **1977**, *66*, 4683−4688.
(16) Armentrout, P. B.; Hodges, R. V.; Beauchamp, J. L. *J. Am. Chem. Soc.* **1977**, *99*, 3162−3163.
(17) Heinemann, C.; Cornehl, H. H.; Schwarz, H. *J. Organomet. Chem.* **1995**, *501*, 201−209.
(18) Marcalo, J.; Leal, J. P.; Pires de Matos, A. *Int. J. Mass Spectrom. Ion Processes* **1996**, *157/158*, 265−274.
(19) Cornehl, H. H.; Wesendrup, R.; Diefenbach, M.; Schwarz, H. *Chem. Eur. J.* **1997**, *3*, 1083−1090.
(20) Gibson, J. K. *Organometallics* **1997**, *16*, 4214−4222.
(21) Gibson, J. K. *J. Am. Chem. Soc.* **1998**, *120*, 2633−2640.
(22) Schumann, H.; Genthe, W. In *Handbook on the Physics and Chemistry of Rare Earths*; Gschneidner, K. A., Jr., Eyring, L., Eds.; Elsevier: New York, 1984; pp 445−571.
(23) Edelmann, F. T. *Angew. Chem., Int. Ed. Engl.* **1995**, *34*, 2466−2488.
(24) Evans, W. J. *Polyhedron* **1987**, *6*, 803−835.
(25) Katz, J. J.; Morss, L. R.; Seaborg, G. T. In *The Chemistry of the Actinide Elements*; Katz, J. J., Seaborg, G. T., Morss, L. R., Eds.; Chapman and Hall: New York, 1986; Vol. 2, pp 1121−1195.
(26) Li, J.; Bursten, B. E. *J. Am. Chem. Soc.* **1997**, *119*, 9021−9032.

S0276-7333(98)00155-1 CCC: $15.00
Publication on Web 05/20/1998

Table 1. M^+ Ground and Lowest Energy "Divalent" Configurations[a]

	ground	"divalent"[b]	ΔE[c]
U^+	$5f^3 7s^2$	$5f^3 6d^1 7s^1$	3
Np^+	$5f^4 6d^1 7s^1$	{GROUND}	0
Pu^+	$5f^6 7s^1$	$5f^5 6d^1 7s^1$	104
Am^+	$5f^7 7s^1$	$5f^6 6d^1 7s^1$	245
Tb^+	$4f^9 6s^1$	$4f^8 5d^1 6s^1$	39
Tm^+	$4f^{13} 6s^1$	$4f^{12} 5d^1 6s^1$	198

[a] An^+: ref 27. Ln^+: ref 28. [b] State with two unpaired, non-f valence electrons outside the rare gas core. [c] Units in kJ mol^{-1}

two non-5f valence electrons capable of forming C−An^+−H intermediates (see Table 1)—accordingly, their high dehydrogenation activities did not illuminate the role of the 5f orbitals. To extend gas-phase organoactinide studies to the transuranium elements, the laser ablation with prompt reaction and detection (LAPRD) technique was developed. Agreement of LAPRD results with those obtained by other methods for the Ln^+ [13] and Th^+ and U^+ [20] established the efficacy of this approach in defining intrinsic M^+ reactivities.

Whereas Np^+, like Th^+ and U^+, exhibits a "divalent" ground-state configuration with two non-5f valence electrons ($[Rn]5f^4 6d^1 7s^1$), Pu^+ requires 104 kJ mol^{-1} to excite from the $[Rn]5f^6 7s^1$ ground state to the $[Rn]5f^5 6d^1 7s^1$ "divalent" state. LAPRD experiments with Np^+ and Pu^+ indicated a substantially reduced alkene dehydrogenation activity for Pu^+ compared with the reactive lighter An^+,[21] indicating chemically inactive 5f electrons and requisite 5f → 6d promotion. On the basis of the energy necessary to excite ground-state Am^+ ($[Rn]5f^7 7s^1$) to the "divalent" $[Rn]5f^6 6d^1 7s^1$ configuration (Table 1), it is predicted that Am^+ should be ineffective at C−H activation and dehydrogenation. The possibility of 5f−6d hybridization in heavy actinide organometallic complexes[26,29] raises the potential for unanticipated reactivity. In the present study, the alkene dehydrogenation efficiency of Am^+ was established by direct comparison with the corresponding reactions for simultaneously ablated Np^+, Tb^+, and Tm^+. $^{237}Np^+$ was selected as a representative reactive An^+ which provided appropriate mass separation from $^{243}Am^+$. The two Ln^+ chosen for comparison with Am^+ were reactive Tb^+ and slightly reactive Tm^+;[13] the latter is appropriate because Tm^+ exhibits a promotion energy roughly comparable to that of Am^+ (Table 1) whereas Eu^+, the lanthanide homologue of Am^+, requires 360 kJ mol^{-1} for promotion.

Gas-phase studies provide the opportunity to identify new organoactinide complexes, the preparation of which is particularly significant for Am because only a few organoamericium compounds have been isolated, including the prototypical Ln-like compound, $Am^{III}(C_5H_5)_3$.[30] Low-valence electrostatically and covalently bonded complexes are more accessible via gas-phase reactions due to the absence of secondary reactants which can attack the unsaturated metal center. The gaseous americium complexes identified in the present study can be compared with the known condensed-phase organometallic compounds of Am and other An.[30−32]

Experimental Section

The transuranium laser ablation mass spectrometer and application of the LAPRD approach to study metal ion−molecule reactions has been described elsewhere,[13,20,21,33] and only key aspects of the experiment are summarized here. Ions were generated by focusing approximately 2 mJ of the output of a XeCl excimer laser onto a ∼0.5 mm^2 spot of a solid target; this corresponded to a nominal average irradiance of $\sim 10^7$ W cm^{-2}, but visual inspection of the ablation plume indicated beam inhomogeneities which presumably resulted in regions of higher irradiance.

For most experiments, the reactant gas was injected into the path of the ablated ions through a constant leak valve, as described previously;[13,20,21] the local reactant pressure was indeterminate but was generally maintained constant, based upon measurement with a remote ion gauge. The pressure was occasionally increased by up to a factor of ∼5 to achieve measurable product ion signals—for M^+ reactivities determined simultaneously by coablation from multicomponent targets, such experimental variations did not affect the comparative reactivity results and comparisons between coablated M^+ were considered the most reliable. For the high vapor pressure reactant, 1-butene, it was found that a pulsed solenoid valve (General Valve Series 9; 0.5 mm orifice) located ∼5 cm from the target provided greater product yields—experiments employing the pulsed valve better established the comparative reactivity of Am^+ with 1-butene. In all cases, the ablated material traveled ∼3 cm through the reactant gas, in a trajectory approximately orthogonal to the flight tube axis; the positive ions from a ∼6 mm^2 cross-sectional cylinder of the propagating ablation plume were injected into the time-of-flight mass spectrometer by a +200 V repeller pulse. The variable time delay between the laser pulse and the repeller pulse, t_d, determined the approximate velocity (kinetic energy) of the sampled ions. Except for the specified reactions with 1-butene, a standard t_d of 35 μs was employed, which typically provided optimal sensitivity to most product ions. This t_d corresponds to collisional energies in the range from ∼10 (for C_2H_4) to ∼40 kJ mol^{-1} (for C_8H_{12}).[21] Experiments carried out using longer t_d corresponded to somewhat lower collision energies, but all of the reactions involved somewhat kinetically hyperthermal metal ions and provided comparable results. It cannot be asserted that fully thermalized ions would exhibit the same reactivities.

The ablation targets were prepared by mixing metal oxide powders with copper powder and compressing the aggregate into a 3 mm diameter pellet at room temperature using a small manual pellet press. The copper, Tb_2O_3, and Tm_2O_3 were commercial products of at least 99.9% purity. The $^{237}NpO_2$ and $^{243}AmO_2$ were archival ORNL samples of at least 99% isotopic purity. The ^{243}Am was produced in the high flux isotope reactor at ORNL; ^{243}Am with its half-life of 7370 years is preferred over the more plentiful ^{241}Am isotope, which has a half-life of only 433 years. The following targets were employed, with the compositions expressed as the atomic percent of each metal constituent: "***Am***" 0.8% Am, 99% Cu; "***Am−Np***" 0.9% Am, 1.8% Np, 97% Cu; and "***Am−Tb−Tm***"

(27) Fred, M. S.; Blaise, J. In *The Chemistry of the Actinide Elements*; Katz, J. J., Seaborg, G. T., Morss, L. R., Eds.; Chapman and Hall: New York, 1986; Vol. 2, pp 1196−1234.
(28) Martin, W. C.; Zalubas, R.; Hagan, L., *Atomic Energy Levels—The Rare-Earth Elements*; NSRDS−NBS 60; National Bureau of Standards (NIST): Washington, DC, 1978; pp 250−254, 358−367.
(29) Bursten, B. E.; Strittmatter, R. J. *Angew. Chem., Int. Ed. Engl.* **1991**, *30*, 1069−1085.
(30) Schulz, W. W.; Penneman, R. A. In *The Chemistry of the Actinide Elements*; Katz, J. J., Seaborg, G. T., Morss, L. R., Eds.; Chapman and Hall: New York, 1986; Vol. 2, pp 887−961.
(31) Marks, T. J.; Streitwieser, A., Jr. In *The Chemistry of the Actinide Elements*; Katz, J. J., Seaborg, G. T., Morss, L. R., Eds.; Chapman and Hall: New York, 1986; Vol. 2, pp 1547−1587.
(32) Marks, T. J. In *The Chemistry of the Actinide Elements*; Katz, J. J., Seaborg, G. T., Morss, L. R., Eds.; Chapman and Hall: New York, 1986; Vol. 2, pp 1196−1234.
(33) Gibson, J. K. *J. Phys. Chem.* **1994**, *98*, 6063−6067, 11321−11330.

0.4% Am, 2.1% Tb, 1.9% Tm, 96% Cu. Each target comprised roughly 1 mg of $^{243}AmO_2$, and only a small fraction (<10%) of each target was ablated during the experiments. The most reliable comparisons between M^+ reactivities by LAPRD were obtained by relating the results for M^+ simultaneously coablated from a multicomponent target—this was the motivation for the ***Am*−*Np*** and ***Am*−*Tb*−*Tm*** targets. The ***Am*** target provided the greatest yield of Am^+, allowing more sensitive detection of potential Am^+ reaction products.

The seven alkene reactants covered a wide range of disposition toward M^+-induced dehydrogenation, which increased in the following approximate order: ethene < *trans*-2-butene ≲ 1-butene < benzene < cyclohexene < 1,3,5,7-cyclooctatetrene ("COT") < 1,5-cyclooctadiene ("COD"). For COT and COD in particular, C−C activation and cracking (e.g., to C_6H_6) could also be significant reaction channels but dehydrogenation via C−H activation was generally dominant and found to be the most reliable and universal indicator of comparative M^+ reactivities. The alkenes were commercial products with the following purities: 99.99% ethene; ≥95% *trans*-2-butene; >99% 1-butene; >99% benzene; 99% cyclohexene; 98% COT; and 99% COD. The latter four liquid reagents were subjected to at least 2 freeze−evacuate−thaw cycles prior to use, and all vapors were introduced into the reaction zone as described above. Only 1-butene was injected via the pulsed valve as well as the constant leak valve, in separate experiments.

Results and Discussion

The results are tabulated as abundances of the complex product ions, $M-L^+$, defined as follows, where "*I*" represents the ion intensity (peak height): $\boldsymbol{A[M^+-L]}\{\boldsymbol{I[M^+-L]/I[M^+]}\} \times 100$. This definition of product abundance is not intended to provide a quantitative measure of the absolute extent of reaction and emphasizes that the LAPRD results provide only a qualitative indication of the comparative reactivities of individual metal and oxide ions; reaction cross sections could not be estimated from these experiments. It should be noted that when **A[M⁺−L]** is large, single-collision conditions likely do not prevail and such a change in reaction processes is presumably a factor in the variability in the results with experimental conditions. Uncertainties in the tabulated abundances are specified in footnote a of Table 2. The nomenclature "**M⁺−L**" is not intended to imply knowledge of the structures or charge distributions of the detected complex ions. For example, "$M^+-C_8H_8$" could correspond to $\{M-C_8H_8\}^+$ and/or $\{C_2H_2-M-C_6H_6\}^+$.[34] The comparative abundances reported in the tables are quantitative for the specified experimental conditions, but it is emphasized that the apparent absolute reactivities varied appreciably depending upon such parameters as the reactant pressure and t_d. However, an essential general observation was that the qualitative order of product abundances remained invariant under all experimental conditions employed. All significant dehydrogenation and adduct products are included in the tables. For COD and COT, cracking could also be significant, and $M^+-C_6H_6$ abundances are included as representative of these channels (other, minor, cracking product abundances were generally in correspondence). The measured abundances and upper limits for undetected products are expressed as comparative M^+ reactivities based upon the following definition: % reactivity of M^+ vs $M'^+ = \{A[M^+-L]/A[M'^+-L]\} \times 100\%$.

Table 2. Product Abundances for Reactions with Butenes, Cyclohexene, and Benzene[a]

	trans-2-butene[b]	
		A[M⁺−C₄H₆]
	Am	
Am⁺		(<0.004)
	Am*−*Np	
Am⁺		(<0.009)
Np⁺		0.45
	Am*−*Tb*−*Tm	
Am⁺		(<0.05)
Tb⁺		1.3
Tm⁺		(<0.13)

	1-butene	
	A[M⁺−C₂H₂]	**A[M⁺−C₄H₆]**
	***Am*−*Np*[c]**	
Am⁺	*d*	(<0.08)
Np⁺	0.12	0.28

	pulsed valve[e]			
	$t_d = 40\ \mu s$	$t_d = 60\ \mu s$	$t_d = 40\ \mu s$	$t_d = 60\ \mu s$
	Am*−*Tb*−*Tm			
Am⁺	*d*	*d*	(<0.3)	(<0.3)
Tb⁺	2.7	440	86	630
Tm⁺	<0.06	<0.4	0.6	23
	Am*−*Np			
Am⁺	*d*	*d*	(<0.7)	(<0.2)
Np⁺	100	13 000	100	1100

	cyclohexene[b]	
	A[M⁺−C₆H₄]	**A[M⁺−C₆H₆]**
	Am	
Am⁺	(<0.0014)	(<0.0014)
	Am*−*Np	
Am⁺	(<0.009)	(<0.009)
Np⁺	0.2	0.8
	Am*−*Tb*−*Tm	
Am⁺	(<0.02)	(<0.02)[f]
Tb⁺	(<0.2)	0.8
Tm⁺	(<0.5)	(<0.5)

	benzene[b]	
	A[M⁺−C₆H₄]	**A[M⁺−C₆H₆]**
	Am*−*Np	
Am⁺	(<0.01)	0.02
Np⁺	0.71	0.18

[a] Abundances, **A[M⁺−L]**, defined in text. Parenthetical values are upper limits for undetected ions. Uncertainties are the greater of 10% or one digit in the last reported significant figure. [b] t_d = 35 μs. [c] t_d = 45 μs. [d] AmC_2H_2 is isobaric with NpO_2 (NpO_2^+ from contamination of the ***Am*−*Tb*−*Tm*** target); it was estimated that **A[Am⁺−C₂H₂] < A[Am⁺−C₄H₆].** [e] All other results are for leak valve; Tb^+ and Np^+ additionally induced double- and triple-dehydrogenation to produce minor $M^+-C_4H_4$ and $M^+-C_4H_2$. [f] Employing a higher pressure of C_6H_{10} and a target spot where only Am^+ was produced, $A[Am^+-C_6H_6] = 0.012$ was measured.

For Np and Tb, substantial amounts of the oxide ions, MO^+, were coablated with the primary M^+ of interest; only minor amounts of TmO^+ and AmO^+ were produced. These oxide yields were in accord with the contrasting dissociation energies: ~500 kJ mol^{-1} for TmO^+ and AmO^+ (estimated) vs ~700 kJ mol^{-1} for TbO^+ and NpO^+.[35−37] Oxygen-abstraction from MO^+ could feasibly account for some of the observed complex ions via reactions such as $MO^+ + C_nH_m \rightarrow M^+-C_nH_{m-2} + H_2O$.

(34) Schroder, D.; Sulzle, D.; Hrusak, J.; Bohme, D. K.; Schwarz, H. *Int. J. Mass Spectrom. Ion Processes* **1991**, *110*, 145−156.

Thermodynamic considerations argue against such reactions for the very stable and abundant oxides such as NpO^+ and TbO^+ [24] but not necessarily for TmO^+ and AmO^+. To illustrate this, the energetics of reaction 1 are evaluated as follows (**L** = 1,3-butadiene; energies in kJ mol^{-1}; thermochemical values from refs 35, 36, and 38):

$$\text{1-butene} + MO^+ \rightarrow M^+{-}L + H_2O \qquad (1)$$

$$\Delta H[\mathbf{(1)}] = \Delta_f H[L] + \Delta_f H[H_2O] - \Delta_f H[O] - \Delta_f H[1{-}\text{butene}] + D[MO^+] - D[M^+{-}L]$$

$$= -381 + D[MO^+] - D[M^+{-}L] \qquad (D = \text{dissociation energy})$$

For NpO^+, $\Delta H[\mathbf{(1)}] \approx 410 - D[Np^+{-}L]$; for TbO^+, $\Delta H[\mathbf{(1)}] \approx 340 - D[Tb^+{-}L]$; and for TmO^+, $\Delta H[\mathbf{(1)}] \approx 100 - D[Tm^+{-}L]$. On the basis of D[AmO] ($\sim$550 kJ mol^{-1})[36] and the yield of ablated AmO^+,[37] $D[AmO^+]$ can be estimated as $\sim$500 kJ mol^{-1}; this estimate implies {IE[Am] − IE[AmO]} $\approx$ 50 kJ mol^{-1}, which is comparable to the corresponding values for lanthanides such as Tm (30 kJ mol^{-1}) and Eu (60 kJ mol^{-1}).[35] Using this approximate $D[AmO^+]$, one obtains $\Delta H[\mathbf{(1)}] \approx 100$ kJ mol^{-1} − $D[Am^+{-}L]$. Considering known $M^+{-}L$ dissociation energies,[4] it is unlikely that the $M^+{-}L$ bond is sufficiently strong to enable reaction 1 for NpO^+ or TbO^+. Although reactions such as eq 1 may be exothermic for AmO^+ and TmO^+ (i.e., $D[M^+{-}L] > 100$ kJ mol^{-1}), these oxide ions were insufficiently abundant to account for the observed $Am^+{-}L$ and $Tm^+{-}L$.

Reactions with Ethene, 1-Butene, and 2-Butene. Ethene was the least reactive substrate employed, and no products were detected for Am^+, Tb^+, or Tm^+ from the ***Am*−*Tb*−*Tm*** target to a limit of $\mathbf{A[M^+{-}L]} < 0.05$. A limit of $\mathbf{A[Am^+{-}L]} < 0.01$ was established using the ***Am*** target. With the ***Am*−*Np*** target it was found that $\mathbf{A[Np^+{-}C_2H_2]} = 0.40$; an upper limit for $\mathbf{A[Am^+{-}C_2H_2]}$ could not simultaneously be determined because $^{243}AmC_2H_2$ is essentially isobaric with $^{237}NpO_2$. In summary, Np^+ exhibited slight reactivity with ethene but the other M^+ were inert to the detection limit (i.e., $\lesssim$10% reactivity vs Np^+).

Representative results for *trans*-2-butene and 1-butene are summarized in Table 2. With *trans*-2-butene, small amounts of $M^+{-}C_4H_6$ were evident for Np^+ and Tb^+ but not for Am^+ or Tm^+. On the basis of the detection limits, it was established that Am^+ was <2% as reactive as Np^+ and <4% as reactive as Tb^+.

The pulsed valve was employed in a series of experiments with 1-butene to provide greater transient reactant pressures in the path of the ablated M^+—this achieved greater product yields and a better measure of the relative reactivity of Am^+ compared with the other M^+. In addition to the dehydrogenation and cracking products specified in Table 2, measurable amounts of oxide ion−alkene condensation adducts were produced in a few of these pulsed-valve experiments (such adducts were generally not detectable under the lower-pressure conditions of the leak-valve experiments). For example, in one case ($t_d = 60\ \mu$s), the following adduct abundances were measured from the ***Am*−*Np*** target: $\mathbf{A[AmO^+{-}C_4H_8]} = 7$; $\mathbf{A[NpO^+{-}C_4H_8]} = 2.5$; $\mathbf{A[NpO_2^+{-}C_4H_8]} = 8$ ($\mathbf{A[MO_n^+{-}L]} \equiv \{\mathbf{I[MO_n^+{-}L]/I[MO_n^+]}\} \times 100$). For $t_d = 60\ \mu$s, Tb^+ and Np^+ reacted very efficiently to produce both the dehydrogenation product, $M^+{-}C_4H_6$, and the cracking product, $M^+{-}C_2H_2$. Additionally, Tm^+ produced a substantial amount of the dehydrogenation product, $Tm^+{-}C_4H_6$, but no $Tm^+{-}C_2H_2$. In sharp contrast, Am^+ remained entirely unreactive, with no $Am^+{-}L$ detected. On the basis of these results for 1-butene, the following comparative dehydrogenation reactivities were established: $Am^+ < 0.002\%$ vs Np^+; $Am^+ < 0.05\%$ vs Tb^+; and $Am^+ < 2\%$ vs Tm^+.

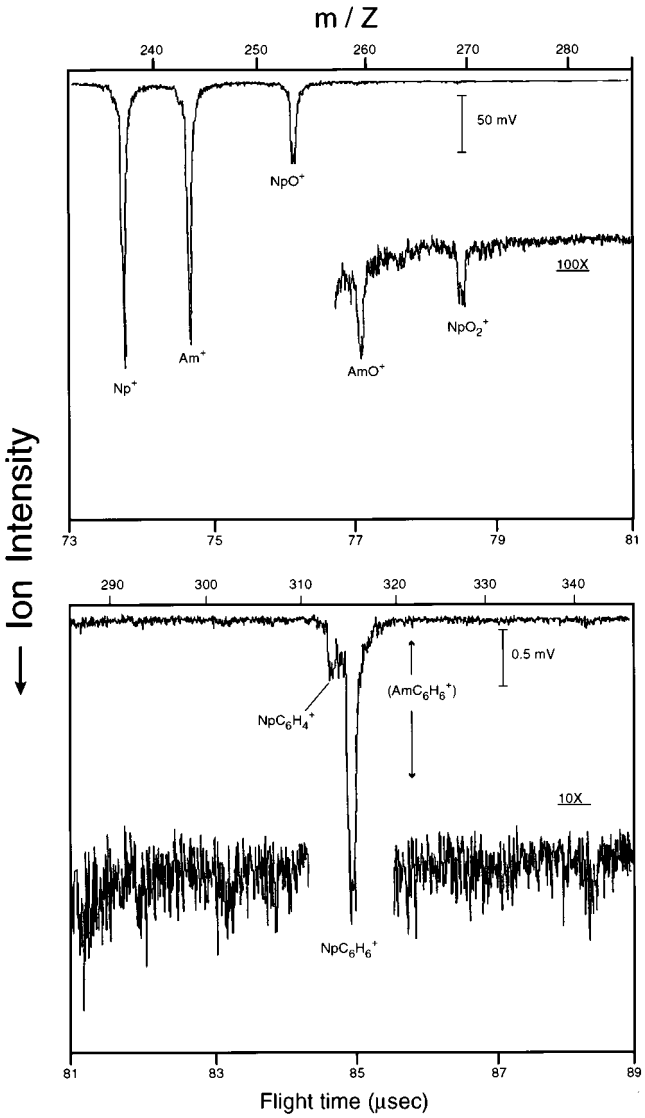

Figure 1. Mass spectrum for ***Am*−*Np*** + cyclohexene.

Reactions with Cyclohexene, Benzene, COD, and COT. The product abundances for reactions with cyclohexene and benzene are given in Table 2, and a mass spectrum for ablation of the ***Am*−*Np*** target into cyclohexene is shown in Figure 1. With cyclohexene, both Np^+ and Tb^+ induced double-dehydrogenation to form $M^+{-}C_6H_6$, presumably benzene complexes. Only Np^+ was sufficiently reactive to effect loss of three H_2 to generate $Np^+{-}C_6H_4$, presumably a benzyne complex. Both Am^+ and Tm^+ were inert toward cyclohexene

(35) Chandrasekharaiah, M. S.; Gingerich, K. A. In *Handbook of the Physics and Chemistry of Rare Earths*; Gschneidner, K. A., Jr., Eyring, L., Eds.; Elsevier: New York, 1989; Vol. 12, pp 409−431.
(36) Haire, R. G. *J. Alloys Compd.* **1994**, *213/214*, 185−190.
(37) Gibson, J. K. *Radiochim. Acta*, in press.

Table 3. Product Abundances for Reactions with COD and COT[a]

	COD (C_8H_{12})	
	A[$M^+-C_6H_6$][b]	**A[$M^+-C_8H_8$]**
	Am	
Am^+	0.03	0.33
	Am−Np	
Am^+	(<0.09)	0.16
Np^+ [c]	1.5	0.7
	Am−Tb−Tm	
Am^+	(<0.02)	0.06
Tb^+ [c]	0.25	0.75
Tm^+	(<0.02)	0.11

	COT (C_8H_8)		
	A[$M^+-C_6H_6$][b]	**A[$M^+-C_8H_6$]**	**A[$M^+-C_8H_8$]**
		Am	
Am^+	0.028	0.043	0.12
		Am−Np	
Am^+	0.06	0.15	0.23
Np^+	0.23	0.23	(<0.05)

[a] See footnote a of Table 2. [b] Abundances for other (minor) cracking products (e.g., $M^+-C_5H_6$) paralleled those for $M^+-C_6H_6$. [c] Also, $\{\mathbf{I[MO^+-C_8H_{10}]/I[MO^+]}\} \times 100 \approx 0.1$ for NpO^+ and TbO^+ (only minuscule AmO^+ and TmO^+ were available for reaction).

within the detection limits, providing the following reactivity limits for Am^+ with this substrate: $Am^+ <$ 1% vs Np^+; $Am^+ <$ 3% vs Tb^+. The ***Am−Np*** target was ablated into benzene, and both Am^+ and Np^+ produced some condensation adduct, $M^+-C_6H_6$. The primary product for Np^+ resulted from dehyrodgenation to $Np^+-C_6H_4$. Within the detection limits, Am^+ was correspondingly inert and a reactivity limit of <1% vs Np^+ was obtained.

The results for reactions with COD and COT are summarized in Table 3, and a mass spectrum for ablation of the ***Am−Tb−Tm*** target into COD is shown in Figure 2. In contrast to the smaller alkenes, all of the M^+—including Am^+—reacted with COD and COT. In the case of COD, cracking to produce $M^+-C_6H_6$, presumably a benzene complex, was the primary reaction channel for Np^+ and secondary channels for both Am^+ (~10% cracking vs dehydrogenation) and Tb^+ (~30% cracking); cracking was not evident for Tm^+ (to <20% relative to dehydrogenation). Although the occurrence of cracking as an alternative reaction channel may obfuscate comparisons of dehydrogenation reactivities based upon the relative abundances of the $M^+-C_8H_8$ product, the following semiquantitative comparisons of dehydrogenation efficiencies were derived from the data in Table 3: $Am^+ \approx 20\%$ vs Np^+; $Am^+ \approx 10\%$ vs Tb^+; and $Am \approx 50\%$ vs Tm^+. Regardless of the quantitative validity of the results, the key conclusion was that Am^+ is effective at dehydrogenating COD, albeit at a somewhat lesser efficiency than for the other M^+. This sharply diverges from the inert character of Am^+ toward the smaller alkenes, as discussed below.

The ***Am*** and ***Am−Np*** targets were ablated into COT, and the primary products were the condensation adduct, $Am^+-C_8H_8$ ($Np^+-C_8H_8$ not detected), the dehydrogenation complexes, $M^+-C_8H_6$, and the cracking complex, $M^+-C_6H_6$. As with COD, Am^+ was substantially reactive when compared with Np^+: $Am^+ \approx 60\%$ dehydrogenation reactivity vs Np^+; $Am^+ \approx 30\%$ cracking reactivity vs Np^+.

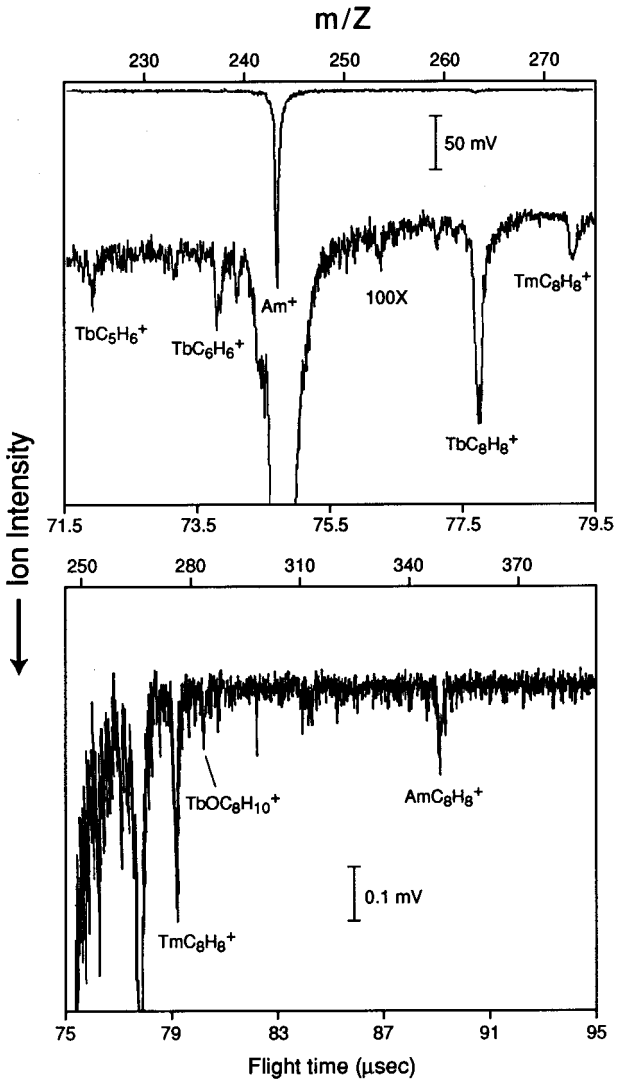

Figure 2. Mass spectrum for ***Am−Tb−Tm*** + COD. At lower mass are peaks attributed to Tb^+ (***I*** = 260 mV), Tm^+ (370 mV), TbO^+ (44 mV) and TmO^+ (0.7 mV).

Summary and Analysis. Focusing on the comparative reactivities of Am^+ vs the other M^+ studied, the above results can be summarized as follows:

(1) With the linear alkenes, Am^+ was apparently inert. Whereas Am^+ was ≪1% as effective at dehydrogenating 1-butene compared with Np^+ and Tb^+, perhaps the most significant finding was that Am^+ was <2% as effective compared with Tm^+.

(2) With both cyclohexene and benzene, Am^+ was also inert, to a limit of <3% for Np^+ and Tb^+. The apparent reaction efficiencies for all four M^+ with the C_6 substrates were small compared with the higher pressure pulsed-valve experiments in which most of the Tb^+ and Np^+ reacted to dehydrogenate 1-butene. For Tm^+ + cyclohexene, no dehydrogenation products were detected; a minuscule amount of $Am^+-C_6H_6$ was measured in only one cyclohexene experiment (Table 2, footnote f). With benzene, a small amount of the $Am^+-C_6H_6$ (presumably benzene) condensation adduct was observed.

(3) With both COD and COT, the reactivity of Am^+ was entirely distinct from that with the smaller alkenes. Specifically, Am^+ appeared to be at least 10% as effective at dehydrogenating COD as were the other three M^+. Similarly, with COT, Am^+ was nearly as effective as Np^+ at dehydrogenation and even exhibited substantial cracking. For Am^+ + COT, the primary product was the condensation adduct, $Am^+-C_8H_8$ (presumably COT).

Unlike experiments such as those carried out with Ln^+ by Cornehl et al.,[11] absolute An^+ reactivities were not determined by LAPRD and quantitative correlation of reactivities with ground-to-divalent promotion energies is, therefore, not possible. However, the qualitative order of reactivities established by the present LAPRD experiments with Am^+ in conjunction with previous studies with Th^+, U^+, Np^+, and Pu^+ [20,21] provide the following ordering of dehydrogenation reactivities: $Th^+ \approx U^+ \approx Np^+ > Pu^+ > Am^+$. This ordering parallels the variations in the An^+ promotion energies and is consistent with a $C-An^+-H$ intermediate which requires two non-5f valence electrons at the metal center for σ-bond formation.

The model for dehydrogenation of hydrocarbons by Ln^+ [11] is one of C−H bond activation by metal ion insertion to produce a $C-Ln^+-H$-activated intermediate; this is presumed to precede facile H_2 loss and complexation of the dehydrogenated product to the liberated Ln^+. It has been demonstrated that the valence 4f electrons of the Ln^+ are ineffective at C−H activation, presumably due to their relatively localized, chemically inert character.[11] Accordingly, those Ln^+ which do not comprise two non-4f valence electrons in their ground-state electronic configurations (e.g., ground Tm^+, $[Xe]4f^{13}6s^1$) must be promoted to a divalent state (e.g., excited Tm^+, $[Xe]4f^{12}5d^16s^1$) with two d/s electrons capable of participating in σ-bonding in the crucial $C-Ln^+-H$-activated complex. As a result, the dehydrogenation reactivities of the Ln^+ directly correlate with the magnitude of the energy necessary to achieve the lowest-lying divalent state. We recently demonstrated a corresponding promotion energy correlation in the actinide series through Pu,[21] suggesting that the 5f electrons are similarly ineffective at σ-bonding in a $C-An^+-H$ intermediate. Extrapolating to the next member of the actinide series, Am^+, a reduced reactivity was predicted based upon the large promotion energy to the lowest-lying divalent state of Am^+ (Table 1).

For the five smallest alkene reactants employed, the comparatively inert behavior of Am^+ is consistent with inactive 5f electrons and the necessity for promotion of a 5f electron to a chemically active 6d orbital. That Am^+ was even less reactive than the relatively inert lanthanide ion, Tm^+ (based upon the 1-butene results), presumably reflects the ~50 kJ mol^{-1} greater promotion energy for Am^+ and indicates effectively no greater C−H activation reactivity of the Am^+ 5f vs the Tm^+ 4f electrons.

Although reactions of Am^+ with COD and COT also revealed somewhat diminished reactivity compared with the other M^+, consistent with the above interpretations, the virtually inert character manifested with the other alkenes was not demonstrated. The substantially enhanced reactivity of Am^+ with COD and COT can be explained by closer examination of possible dehydrogenation mechanistics. The simplified activation model posited above is essentially based on preparation of a free divalent M^+ which inserts into the target C−H bond of the reactant substrate. Although this model describes the qualitatively constant comparative reactivities well, the widely disparate absolute reactivities obtained for different substrates can be rationalized by a more detailed consideration of the dehydrogenation process.

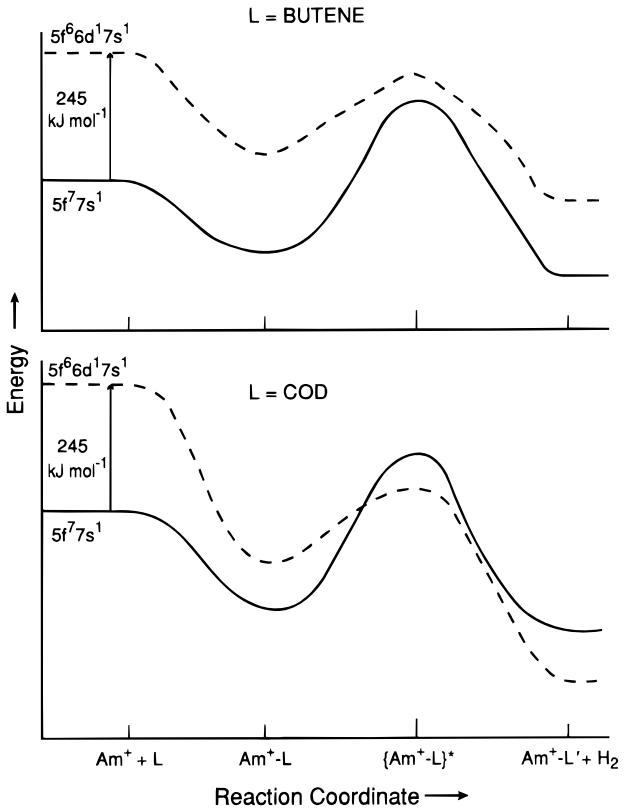

Figure 3. A postulated qualitative curve-crossing[11] representation of one possible explanation why Am^+ dehydrogenates COD but not butene. The solid lines represent the conjectured pathways for ground-state Am^+ ($[Rn]5f^77s^1$) and the dashed lines those for "divalent" excited-state Am^+ ($[Rn]5f^66d^17s^1$); the comparative energetics may be exaggerated to emphasize distinctions. It should also be noted that a factor facilitating COD dehydrogenation is that the initial Am^+-COD adduct is probably longer-lived than the Am^+-butene adduct.

Dehydrogenation should be considered to proceed via interaction of an initially ground-state M^+ with the hydrocarbon substrate, L, rather than by reaction of a free prepared divalent M^+ with L. As ground M^+ approaches L, the electronic structures of both moieties will be perturbed and insertion of M^+ into the target C−H bond can be envisioned as proceeding by a "curve-crossing" mechanism such as that invoked by Cornehl et al.[11]—this model retains the correlation with M^+ excitation energies. A postulated reaction pathway for the dehydrogenation of COD by Am^+ is shown in Figure 3—the relative energy levels in comparison with the corresponding noncrossing butene curves are highly qualitative and probably exaggerated. The reaction is conjectured to proceed through the following key stages: (1) isolated Am^+ + L (L = reactant alkene); (2) an Am^+-L adduct; (3) an activated intermediate, $\{Am^+-L\}^*$; and (4) the $Am^+-L' + H_2$ products (L′ = dehydro-

genated alkene). In contrast to monoenes such as butene, polyenes (particularly cyclic polyenes) offer multiple π-bond sites for strong electrostatic and/or covalent bonding with a metal ion, and the bonding between M^+ and a polyene is generally expected to be stronger than that between M^+ and a monoene. This generalization is supported by measured and estimated M^+-L dissociation energies;[4] results from the present study provide circumstantial substantiation in that condensation adducts, M^+-L, were detected only with benzene and COT. Accordingly, the stability of a Am^+-COD adduct is predicted to be greater than that of a Am^+-butene adduct, as indicated by the depths of the Am^+-L wells in Figure 3. Additionally, the large COD ligand should better accommodate the internal energy released in the formation of the initial adduct complex, resulting in a longer lifetime and enhanced opportunity for the subsequent insertion/elimination processes. Furthermore, it is postulated that the $5f^6 6d^1 7s^1$ configuration, with its two electrons in extended valence orbitals, should exhibit a stronger covalent interaction with alkenes (particularly polyenes) compared with the $5f^7$-$7s^1$ configuration—this hypothesis is also reflected in the depths of the Am^+-L wells in Figure 3. In contrast, the electrostatic attraction between Am^+ and the reactants should be greater for ground-state Am^+ ($5f^7 7s^1$) due to decreased repulsive interactions absent in a relatively spatially extended 6d electron; highly excited Am^+ [$5f^8 6d^0 7s^0$] would be expected to exhibit minimal repulsive interactions. On the basis of these presumptions, which have been incorporated into Figure 3, it might be understood why Am^+ should be unreactive with butene—no curve-crossing—but somewhat reactive with COD where there may be curve-crossing. Following elimination of the first H_2 (Figure 3), the Am^+ complexed to C_8H_{10}, presumably cyclooctatriene, apparently readily inserts into one of the two remaining allylic C−H bonds to induce the second H_2 loss and produce the primary product, $Am^+-C_8H_8$ (no $M^+-C_8H_{10}$ were detected).

The potential energy surface of the Am^+ + COD reaction coordinate could feasibly be additionally affected by 5f-bonding interactions. Although the degree of 5f orbital participation in organoactinide bonding almost certainly diminishes across the An series, some (minor) 5f interaction might be anticipated with Am (and even heavier An).[39] Greater interaction with π-electron-rich substrates such as COD of the $5f^6$ subshell of excited Am^+, with its vacant 5f orbital, might be expected when compared with the especially stable half-filled $5f^7$ subshell of ground-state Am^+. Such 5f bonding could contribute to the stabilization of the Am^+-COD intermediate adduct and further deepen the Am^+-COD energy well (Figure 3), thereby facilitating C−H activation via the curve-crossing mechanism. Among the few Am organometallics which have been isolated is $KAm(COT)_2$,[30,31] and the potential for 5f bonding—either by direct interaction with the π orbitals of COD or as components of Am^+ hybrid bonding orbitals[29] remains a plausible partial explanation of the exhibited gas- and condensed-phase organometallic chemistry of americium. It is notable that a covalent interaction between the 4f orbitals of Eu, the lanthanide homologue of Am, and the C_5H_5 ligands has been postulated for $(C_5H_5)_3Eu^{III}(THF)$ based upon Mossbauer spectroscopy.[40] The proposed bonding interaction of the usually localized 4f orbitals was attributed to a nephelauexetic effect of the ligands, which effectively expands these orbitals. The 5f orbitals are inherently more extended than the 4f orbitals, and a π-electron-rich ligand such as COD could induce a corresponding nephelauexetic expansion, which would facilitate enhanced 5f orbital−ligand bonding.

Conclusions

With respect to dehydrogenation (C−H activation) of small linear alkenes, cyclohexene and benzene, Am^+ is essentially inert compared with Np^+, Tb^+, and even the relatively unreactive lanthanide ion Tm^+. Although Am^+ was also less reactive than the other three M^+ with COD and COT, the discrepancy was much smaller. The greater reactivity with these larger cyclic polyenes can be rationalized in the context of a stronger Am^+-ligand bonding interaction, a longer-lived adduct, and the availability of easily cleaved allylic bonds in the target alkene. This model invokes a curve-crossing energy surface and admits the possibility of 5f-ligand interactions which could participate in the stabilization of transient adduct intermediate complexes. Spectroscopic studies are needed to directly probe the character—localized or partially bonding—of the 5f electrons in these complexes.

The results confirm that the technique of LAPRD consistently provides experimental results which can be interpreted in the context of the comparative energies needed to excite a ground-state f-element M^+ from a configuration comprising only one non-f valence electron to a "divalent" configuration comprising two such valence electrons. Regardless of the possible role of the 5f electrons in stabilizing the An^+-L complexes via interaction with the alkene π orbitals, the previous results for Pu^+ and present results for Am^+ indicate that the 5f electrons are ineffective at forming σ-bonds in the $C-An^+-H$ intermediate.

Acknowledgments. This work was sponsored by the Division of Chemical Sciences, Office of Energy Research, U.S. Department of Energy, under Contract DE-AC0596OR22464 at Oak Ridge National Laboratory with Lockheed Martin Energy Research Corp. The ^{243}-Am used in this study was supplied by the Division of Chemical Sciences, Office of Energy Research, U.S. Department of Energy through the transplutonium element production facilities located at the Oak Ridge National Laboratory.

OM9801554

(38) Ion Energetics Data. In *NIST Standard Reference Database Number 69*; Mallard, W. G.; Linstrom, P. J., Eds.; National Institute of Standards and Technology: Gaithersburg, MD (http://webbook.nist.gov), August, 1997.

(39) Strittmatter, R. J.; Bursten, B. E. *J. Am. Chem. Soc.* **1991**, *113*, 552−559.

(40) Depaoli, G.; Russo, U.; Valle, G.; Grandjean, F.; Williams, A. F.; Long, G. J. *J. Am. Chem. Soc.* **1994**, *116*, 5999−6000.